Synthesis and properties of novel blue-emitting materials: anthracene-based derivatives

Gang Shi (石 刚)*, Jinguo Wang (王晋国), Chunlong Xu (徐春龙), Xiaoting Li (李晓婷), and Zhen Wang (王 真)

School of Science, Chang'an University, Xi'an 710064, China
**Corresponding author: shigang_xa@126.com*

Received January 6, 2015; accepted February 12, 2015; posted online March 18, 2015

Two kinds of novel blue-emitting materials, anthracene-based derivatives, are synthesized by the Suzuki coupling reaction. It is worth noting that the maximum emission wavelengths of the two materials are 441 and 444 nm in tetrahydrofuran and 456 and 454 nm in film states, which are the typical blue fluorescence and the fluorescence quantum yields of them are 0.87 and 1.12 by using 9,10-diphenylanthracene ($\Phi_f = 0.90$) as a calibration standard. The full width at half maximum of them are 56, 55 nm in solution, respectively, presenting good color purity. Both of them display superior thermal properties and electrochemical properties. Scanning electronic microscope results show that the films of two compounds are continuous, compact, and smooth after 100°C for 3 h. These data indicate their potential to be prepared for high efficiency and long operation lifetime organic light-emitting diodes devices.

OCIS codes: 230.3670, 160.2540, 160.4890.
doi: 10.3788/COL201513.042301.

Organic light-emitting diodes (OLEDs) have emerged as the most promising next-generation flat-panel display technology in the decades since the pioneering work of Tang and Vanslyke[1]. They have more advantages, such as fast response, low voltage driver, and wide viewing angle compared with traditional displays[2–5].

Full-color displays require red-, green-, and blue-emitting materials of relatively high stability, efficiency, and color purity. Although significant improvements in OLED performance have been achieved over the past decades, the highest efficiency reported for deep-blue fluorescent OLEDs is about 7%, while that for deep red devices is over 17% and for green is over 21%[6–8]. Moreover, few of them exhibit stable thermal stability and morphological stability in OLEDs owing to their crystallization and low glass transition temperature (T_g)[9]. Therefore, blue-emitting materials having all the attributes of high electroluminescent efficiency, a long operation lifetime, and good color purity are required.

9,10-di(2-naphthyl)anthracene (ADN) is a major blue-emitting material that was first developed by Kodak[10], realizing a blue luminance efficiency of 3.5 cd/A and a half-life of 4000 h with initial light output at 700 cd/m^2, presenting good optical properties and high efficiency. However, it is also reported that the film forming properties of ADN are not acceptable. The thin film of ADN is found to be morphologically unstable, and could accelerate the decay about a lifetime of the device[11,12]. Hence, it is necessary to improve the properties of blue-emitting materials' anthracene-based derivatives.

In this work, we designed and synthesized two kinds of anthracene-based compounds, 2-(4-t-butylphenyl)-5-(4-(2-(9,10-di(β-naphthyl))anthracene-yl)-phenyl)-1,3,4-oxadiazole(β-ADN-2-PBD) and 3-(4-t-butylphenyl)-5-(4-(2-(9,10-di(β-naphthyl))anthracene-yl)biphenyl)-4-phenyl-1,2,4-triazole (β-ADN-2-TAZ). Both of them show high fluorescence quantum efficiency, and thermal and morphological stability. Herein, we report the synthesis and properties of the two compounds.

All reagents and solvents used in the experiments were analytically pure. Tetrahydrofuran (THF) was purified by distillation from sodium in the presence of benzophenone. UV–vis absorption and emission spectra were measured using a Unico UV-4802 double beam spectrophotometer and a 970CRT fluorescence spectrophotometer, respectively. Thermal properties were performed by a TA DSC Q20 device and a TA TGA 2950 thermal analyzer at a heating rate of 10°C/min. Using $AgNO_3$/Ag and platinum wire as the reference and counter electrodes, electrochemical properties were measured by a CHI660D analyzer with the electrolyte of an Ar-saturated 0.1 mol/L n-Bu_4NPF_6 solution in anhydrous CH_2Cl_2 and a scanning rate of 0.1 V/s. Scanning electron microscopy was carried out by the U.S. FEI Company 600 Quanta FEG scanning electron microscope (SEM) instrument.

The synthesis routes of the two compounds were sketched in Scheme 1 and Scheme 2. Compounds **1** and **7** were first synthesized according to Refs. [13,14]. Compounds **2** and **4** were synthesized by reacting **1** and 4-tert-butylbenzoyl hydrazine, respectively, with aniline at 0°C for 3 h. The dehydration of compound **2** afforded compound **3**. At the same time, the acylation action of compound **4** afforded compound **5**, which when mixed with 4-tert-butylbenzoyl hydrazine at 120°C for 4 h in dimethylacetamide could produce compound **6**. Meanwhile, the transformation of compound **7** into boronic acid **8** was performed by lithium–bromide exchange at—78°C, followed by reaction with triisopropyl borate at—78°C

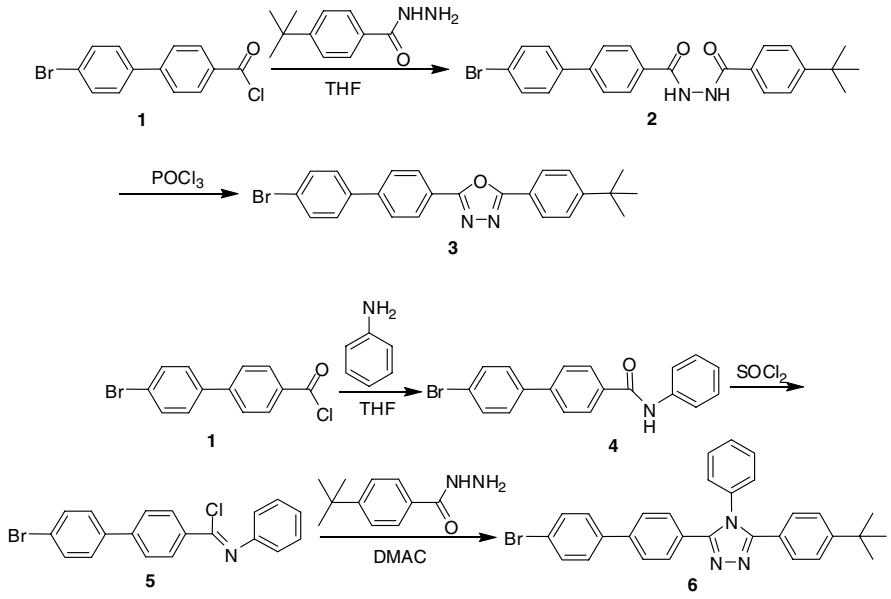

Scheme 1. Synthesis routes of two intermediates.

and hydrolyzed in hydrochloric acid at room temperature. Finally, the $Pd(PPh_3)_4$-catalyzed Suzuki cross-coupling reactions between compound **8** and compounds **3** and **6** afforded the desired anthracene-based derivatives in yields of 86.7% and 80.2%, respectively. All the intermediates and the final products were purified by recrystallization or column chromatography, and the new compounds (β-ADN-2-PBD and β-ADN-2-TAZ) were characterized with ^{1}H NMR, ^{13}C NMR, elemental analysis, and ESI mass spectroscopy.

β-ADN-2-PBD: ^{1}H NMR ($CDCl_3$, 500 MHz) δ (ppm): 8.17 (d, $J = 8.55$ Hz, 2 H), 8.12 (d, $J = 8.30$ Hz, 2 H), 8.06 (t, $J = 8.60$ Hz, 6 H), 8.02 (s, 1 H), 7.96 (d, $J = 7.65$ Hz, 2 H), 7.86 (d, $J = 9.10$ Hz, 1 H), 7.66-7.75 (m, 7 H), 7.63 (s, 8 H), 7.55 (d, $J = 8.60$ Hz, 2 H), 7.32-7.34 (q, 2 H), 1.37 (s, 9 H). ^{13}C NMR ($CDCl_3$, 500 MHz) δ (ppm): 164.7,

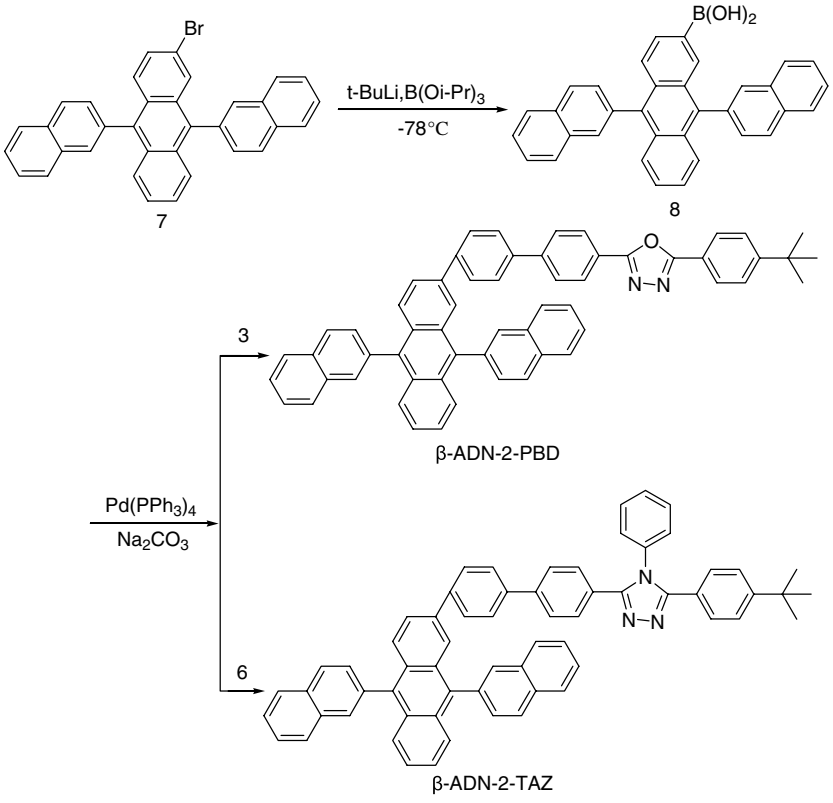

Scheme 2. Synthesis routes of two compounds.

164.3, 150.1, 143.1, 139.9, 138.9, 137.5, 134.3, 134.2, 134.1, 133.7, 133.6, 132.7, 128.8, 128.6, 128.4, 128.3, 128.1, 128.0, 127.1, 126.4, 126.3, 126.2, 125.6, 125.1, 124.9, 124.8, 123.1, 34.5, 31.3. Anal. Calc.: C, 88.97; H, 5.41; N, 3.58. Found: C, 88.79; H, 5.44; N, 3.66. MS (ESI), m/z: Calc.: 782.33, Found: 782.65 [M^+].

β-ADN-2-TAZ: ^{1}H NMR ($CDCl_3$, 500 MHz) δ (ppm): 8.11 (d, $J = 8.00$ Hz, 2 H), 7.93-8.05 (m, 6 H), 7.84 (d, $J = 9.15$ Hz, 2 H), 7.72-7.78 (m, 2 H), 7.60-7.68 (m, 7 H), 7.52-7.57 (q, 4 H), 7.43-7.49 (m, 8 H), 7.36 (d, $J = 8.55$ Hz, 2 H), 7.30-7.33 (m, 4 H), 7.21 (d, $J = 8.70$ Hz, 2 H), 1.28 (s, 9 H). ^{13}C NMR ($CDCl_3$, 500 MHz) δ (ppm): 155.5, 155.3, 149.8, 142.9, 139.6, 138.3, 137.1, 134.3, 134.2, 134.0, 133.7, 133.6, 132.7, 129.9, 129.7, 129.2, 128.8, 128.6, 128.4, 128.3, 128.1, 128.0, 127.0, 126.4, 126.3, 126.2, 125.6, 125.1, 124.9, 124.8, 34.8, 31.4. Anal. Calc.: C, 89.58; H, 5.52; N, 4.90. Found: C, 89.29; H, 5.55; N, 4.90. MS (ESI), m/z: Calc.: 857.38, Found: 857.33 [M^+].

The UV–vis absorption spectra of the compounds in THF at 2×10^{-5} mol/L and film states are shown in Fig. 1, and the corresponding photophysical data are summarized in Table 1. The absorption spectra can be divided into three regions: the intense absorption bands at higher energy (240–260 nm) are assigned to the electronic transition ($\pi - \pi^*$) of the aryl group[15], 300–350 nm shows the electronic transition ($\pi - \pi^*$) of the oxadiazole group and triazole group[16], 350–450 nm shows the characteristic vibrational patterns of an isolated anthtacene group. The absorption spectra of two compounds in film states have a redshift of 1–3 nm compared with that in solution. According to the equation [$Eg = 1240/\lambda_{ON}(nm)$], the optical energy bandgap is 2.88 eV for β-ADN-2-PBD, and 2.89 eV for β-ADN-2-TAZ, respectively.

At the excitation wavelength of 390 nm, the photoluminescence (PL) maximum is 444 nm, 456 nm for β-ADN-2-PBD, and 441 and 454 nm for β-ADN-2-TAZ in solution and films, respectively, which are the typical blue fluorescence. The full width at half maximum (FWHM) is 56 nm for β-ADN-2-PBD and 55 nm for β-ADN-2-TAZ, while that of ADN is 57 nm, presenting good color purity. The fluorescence quantum yields are 0.87 and 1.12 by using 9,10-diphenylanthracene ($\Phi_f = 0.90$) as a calibration standard[17], respectively.

The thermal properties of β-ADN-2-PBD and β-ADN-2-TAZ were investigated by differential scanning

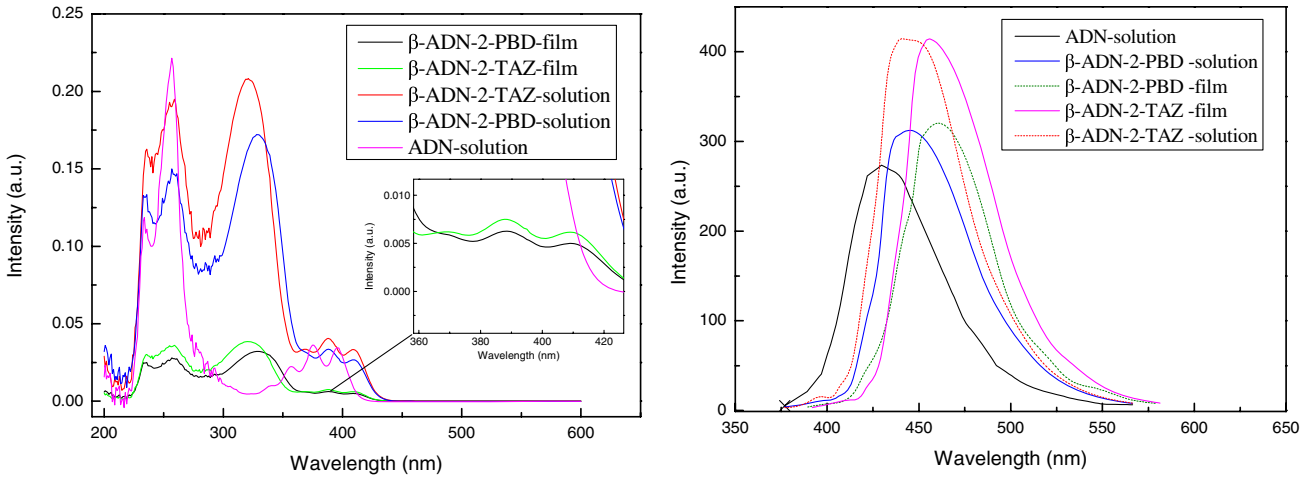

Fig. 1. UV–vis (L) and PL (R) spectra of β-ADN-2-PBD, β-ADN-2-TAZ, and ADN.

Table 1. Photophysical and Thermal Properties of ADN, β-ADN-2-PBD, and β-ADN-2-TAZ

	Absorption (nm)		PL[b](nm)			
Compounds	solution[a]	film	solution	film	Φ_f[c]	T_g/[d]T_m/[d]T_d[e] (°C)
ADN[f]	234, 257, 357, 375, 396	—	430	—	0.80	—/388/397
β-ADN-2-PBD	236, 261, 328, 369, 388, 409	239, 263, 330, 370, 388, 410	444	456	0.87	—/334/440
β-ADN-2-TAZ	237, 266, 322, 369, 388, 409	240, 268, 325, 370, 389, 410	441	454	1.12	175/ > 350/459

[a]Measured in THF.
[b]Excited at 390 nm.
[c]Fluorescence quantum yields were determined by using 9,10-diphenylanthracene ($\Phi_f = 0.90$) as a calibration standard excited at 390 nm.
[d]Obtained from DSC measurement.
[e]Obtained from TGA measurement (temperature at 5% weight loss under nitrogen, 10°C/min ramp rate).
[f]The thermal data for ADN come from Ref. [17].

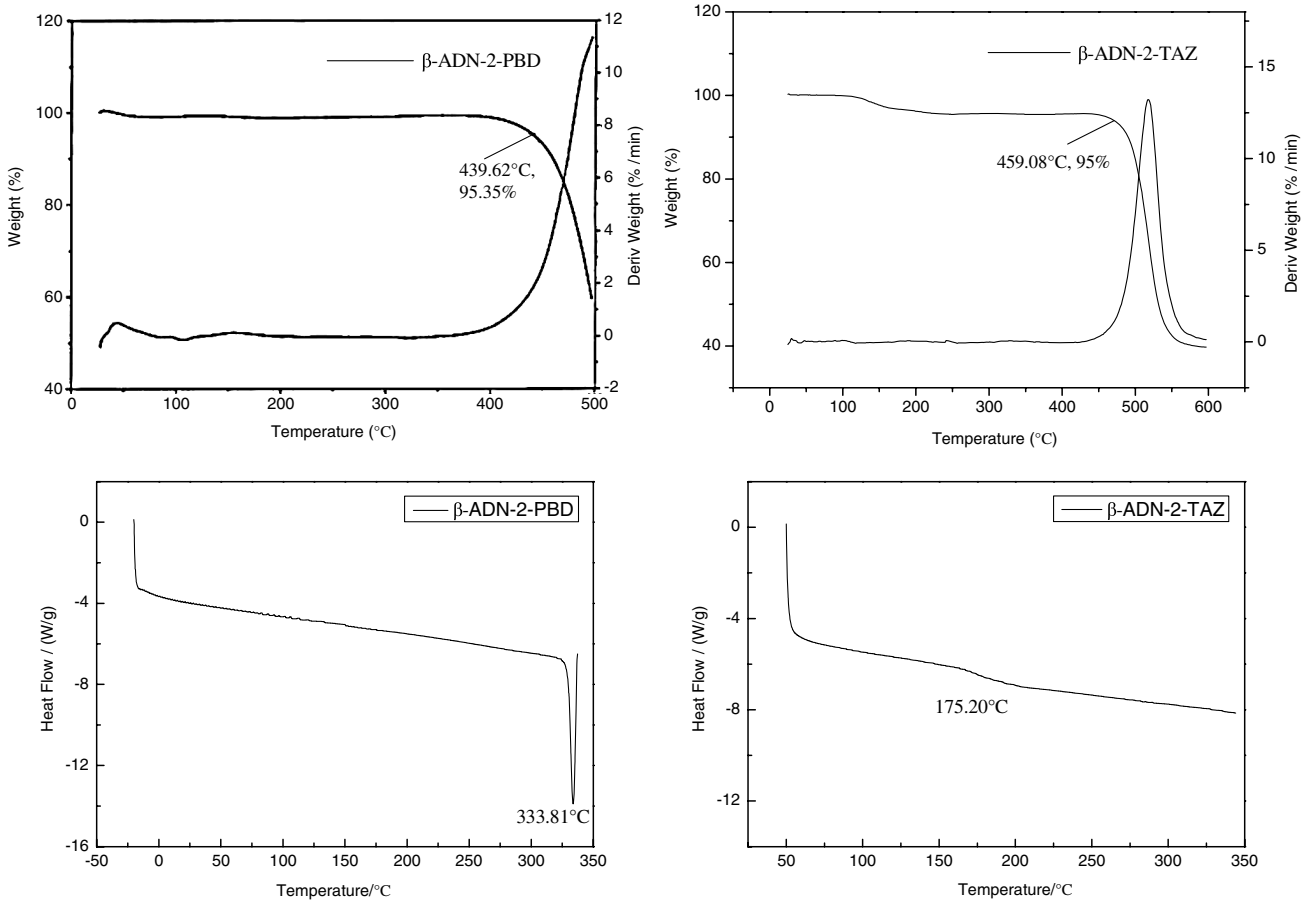

Fig. 2. TGA and DSC traces of β-ADN-2-PBD and β-ADN-2-TAZ

calorimetry (DSC) and thermogravimetric analyses (TGA). The relevant data of glass of transition temperature T_g, melting transition temperature T_m, and decomposition temperature T_d are shown in Fig. 2 and Table 1. In Fig. 2, β-ADN-2-TAZ presents a glass transition temperature T_g of 175°C, which is higher than those of most of the well-known small molecule materials used in optoelectronic fields[18]. In the case of β-ADN-2-PBD, T_g could not be observed while the melting transition temperature (T_m) was observed at 334°C. As a result, β-ADN-2-PBD and β-ADN-2-TAZ have good thermal stability despite being relatively low molecular weight organic compounds.

The electrochemical properties of β-ADN-2-PBD and β-ADN-2-TAZ were studied by cyclic voltammetry. The results are shown in Fig. 3 and Table 2. The bandgap (E_g) was calculated from the absorption edges [$Eg = 1240/\lambda_{ON}$ (nm)]. The highest occupied molecular orbital (HOMO) and lowest unoccupied molecular orbital (LUMO) of the materials were determined by the equation $HOMO(eV) = -(E_{ox} + 4.8\ eV)$. The LUMO levels were calculated by subtracting the bandgap from the HOMO levels. The HOMO, LUMO, and bandgap of these two

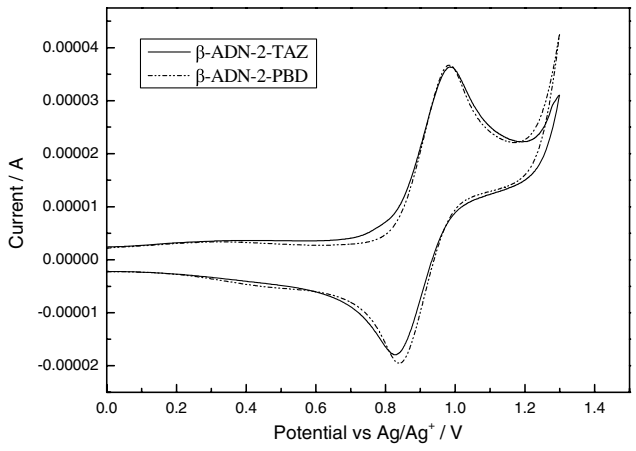

Fig. 3. *I-V* curves of β-ADN-2-PBD and β-ADN-2-TAZ.

Table 2. Electrochemical Properties of ADN, β-ADN-2-PBD, and β-ADN-2-TAZ

Compound	Eox(V)	λ_{ON} (nm)	E_g (eV)	E_{HOMO} (eV)	E_{LUMO} (eV)
ADN[a]	—	420	2.95	−5.60	−2.65
β-ADN-2-PBD	0.81	430	2.88	−5.61	−2.73
β-ADN-2-TAZ	0.74	429	2.89	−5.54	−2.65

[a]Electrochemical data of ADN come from Ref. [19].

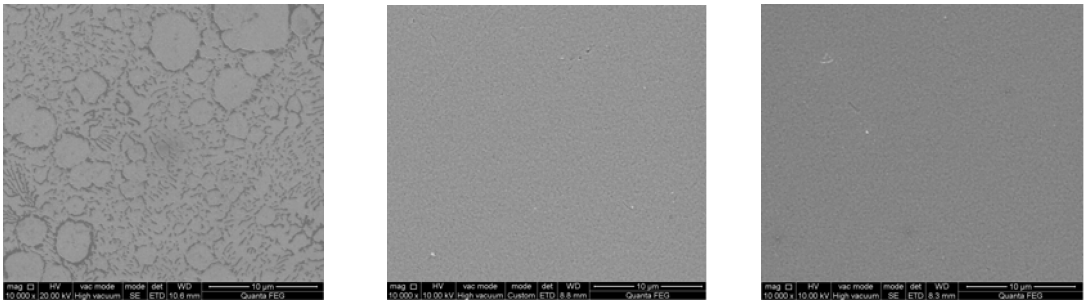

(a) (b) (c)

Fig. 4. SEM images of (a) ADN, (b) β-ADN-2-PBD and (c) β-ADN-2-TAZ.

materials are close to that of ADN, showing that β-ADN-2-PBD and β-ADN-2-TAZ are very suitable not only for blue-emitting materials but also for blue host materials.

Morphologies of ADN, β-ADN-2-PBD, and β-ADN-2-TAZ were studied by a SEM, and the images are shown in Fig. 4. The thin films were spun on indium tin oxides glass with a rotation rate of 800 rpm and a rotation time of 12 s, 3 h under vacuum at 100°C.

Figure 4 shows that the ADN film is discontinuous, and there are some islands separated by gaps, which is consistent with the report in Ref. [20], while the films of two compounds are continuous, compact, and smooth after 100°C for 3 h, which is probably because the introduction of bulky moieties into the 2-position of anthracene improves the morphological stability[21,22].

In conclusion, two kinds of novel blue-light-emitting anthracene-based derivatives are synthesized. It is interesting that introduction of PBD, TAZ branches to ADN can obtain higher fluorescence quantum yields. At the same time, both of them have good color purity, superior thermal stabilities, and continuous, compact, smooth films after 100°C for 3 h. It has significant potential to prepare for high efficient and long operation lifetime OLEDs.

This work was supported by the National Natural Science Foundation (NNSF) of China (No. 51101022) and the Science and Technology Research Projects of Shaanxi Province (No. 2013K06-27).

References

1. C. W. Tang and S. A. VanSlyke, Appl. Phys. Lett. **51**, 913 (1987).
2. C. W. Tang, S. A. VanSlyke, and C. H. Chen, J. Appl. Phys. **65**, 3610 (1989).
3. J. A. Yoon, Y. H. Kim, C. G. Jhun, S. E. Lee, Y. K. Kim, F. R. Zhu, and W. Y. Kim, Chin. Opt. Lett. **12**, 012302 (2014).
4. C. Chen, H. Li, Y. Zhang, C. Moon, W. Y. Kim, and C. G. Jhun, Chin. Opt. Lett. **12**, 022301 (2014).
5. S. Huang, Z. Ye, J. Lu, Y. Su, C. Chen, and G. He, Chin. Opt. Lett. **11**, 062302 (2013).
6. Q. Wang, J. Yu, J. Zhao, J. Wang, M. Li, and Z. Lu, J. Lumin. **134**, 870 (2013).
7. G. Zhang, H. H. Chou, X. Jiang, P. Sun, and C. H. Cheng, Org. Electron. **11**, 632 (2010).
8. X. Zhang, J. Lin, X. Ouyang, Y. Liu, X. Liu, and Z. Ge, J. Photochem. Photobiol. A **268**, 37 (2013).
9. K. R. Wee, W. S. Han, J. E. Kim, A. L. Kim, S. Kwon, and S. O. Kang, J. Mater. Chem. **21**, 1115 (2011).
10. J. Shi and C. W. Tang, Appl. Phys. Lett. **80**, 3201 (2002).
11. E. M. Han, L. M. Do, N. Yamamoto, and M. Fujihira, Thin Solid Films **273**, 202 (1996).
12. M. T. Lee, H. H. Chen, C. H. Liao, C. H. Tsai, and C. H. Chen, Appl. Phys. Lett. **85**, 3301 (2004).
13. V. W. Yam, W. K. Lee, and K. K. Cheung, J. Chem. Soc. **11**, 2335 (1996).
14. Q. L. Xu, H. Y. Li, C. C. Wang, and S. Zhang, Inorg. Chem. **391**, 50 (2012).
15. Y. H. Kim, H. C. Jeong, S. H. Kim, K. Yang, and S. K. Kwon, Adv. Funct. Mater. **15**, 1799 (2005).
16. U. Manabu, I. Takenori, and N. Takaharu, Chem. Mater. **13**, 2680 (2001).
17. M. H. Ho, C. M. Chang, and T. M. Chen, Org. Electron. **9**, 101 (2008).
18. S. A. VanSlyke, C. H. Chen, and C. W. Tang, Appl. Phys. Lett. **69**, 2160 (1996).
19. G. J. Bie, S. Y. Cai, B. Liu, R. Zhou, Y. N. Xue, and Q. N. Liu, Chin. J. Liq. Cryst. Disp. **22**, 301 (2007).
20. H. Y. Jiang, M. L. Xu, X. C. Song, R. Zhou, and J. Tian, Opt. Mater. **35**, 89 (2012).
21. K. Danel, T. H. Huang, J. T. Lin, Y. T. Tao, and C. H. Chuen, Chem. Mater. **14**, 3860 (2002).
22. I. Cho, S. H. Kim, J. H. Kim, S. Park, and S. Y. Park, J. Mater. Chem. **22**, 123 (2011).